15TH IEA HEAT PUMP CONFERENCE
MAY 26–29, 2026 | HOFBURG
VIENNA 2026
DECARBONISATION THROUGH INNOVATION

Performance assessment and geometric design of a steam compressor for an R718 high-temperature heat pump within the GEOSYN project

Ole Marius Moen[a*], Joshua Dowdell[a], Sigurd Sannan[a], Krzysztof Banasiak[a], Lorenzo Talluri[b], Andrea Zini[b], Adriano Milazzo[b], Andrea Rocchetti[b], Vaishak Somasundaram[c], Paride Gullo[c], Giuseppe Vitri[d], Filippo Luchetti[d], Mauro Dallai[e]

[a]SINTEF Energy Research, Department of Thermal Energy, Trondheim, 7034, Norway
[b]University of Florence, Department of Industrial Engineering, Florence, 50139, Italy
[c]University of Southern Denmark, Institute of Mechanical and Electrical Engineering, Sønderborg, 6400, Denmark
[d]Rivacold S.r.l, Vallefoglia, 61022, Italy
[e]Officine Mario Dorin S.p.A., Florence, 50061, Italy

Abstract

Industrial process heating is dominated by fossil-based energy sources, making energy consumption in this sector extremely carbon intensive. High-temperature heat pumps (HTHPs) represent an attractive technology to replace fossil-based heat production, enabling decarbonization combined with improved energy efficiency. This paper presents the evaluation of a 4-stage piston compressor geometry for a steam-based HTHP for different cycle layouts, designed for a temperature lift of 80 K and producing steam at 200 °C and 15.5 bara. The study is performed within the GEOSYN Horizon Europe project. The development of a novel compressor using steam as the working fluid, consisting of four compression stages, introduces design challenges related to correct sizing of the cylinder geometry to optimize COP, while also satisfying constraints such as maximum discharge temperatures and the need for interstage steam bypass or recycling in different cycle layouts. The evaluation of different methods for interstage steam desuperheating and their impact on the compressor geometry is presented. Dynamic modelling of the HTHP has been carried out to investigate the operational performance under various conditions and constraints, from start-up using air as the working fluid to steady-state operation with steam. The results support the development of the overall system design and operational strategy of the HTHP, as well as the dimensioning of key components.

Selection and/or peer-review under the responsibility of the organizers of the 15th IEA Heat Pump Conference 2026.

Keywords: High Temperature Heat Pump; steam, piston compressor; dynamic modeling; industrial process heating;

1. Introduction

Industrial process heat accounts for a large share of global final energy use, around 25% (≈105 EJ). Fossil fuels still dominate industrial heat supply with a share of about 90%, making the sector responsible for 23% of global energy-related CO2 emissions [1]. Decarbonizing these energy streams is therefore essential for meeting climate targets. Roughly 20% of the industrial heat demand is required at temperatures between 100–200 °C [1]. In this temperature range, technologies such as high-temperature heat Pumps (HTHPs) are gaining increasing research and industrial attention as a route to decarbonization combined with improved energy efficiency.

* Corresponding author. Tel.: +47 454 50 516
E-mail address: ole.moen@sintef.no

However, several barriers still limit the widespread implementation of HTHPs – both economic, due to the large investment costs, and technical, due to high-temperature compressor operation leading to material, sealing and lubrication challenges [2,3]. Over the past decade, research and demonstration activities have advanced rapidly. Numerous national and European collaborative projects have played a central role in maturing the field through the development of components, cycle concepts, and industrial pilots capable of delivering 150–200 °C process heat [5–9]. This development is also showcased by IEA HPT Annex 58, which highlights a growing number of HTHP suppliers entering the market with a wide variety of technologies [3]. Research and development on HTHPs using natural working fluids has gained significant traction in recent years and now seems to dominate over low-GWP synthetic refrigerants, although some HFOs still remain attractive in certain applications [3,8].

Among the natural working fluids, water (R718) is receiving increasing attraction, with steam-based R718 cycles now being developed and installed in top-cycle configurations, such as mechanical vapor recompression (MVR) and in single-fluid cycles utilizing heat sources above 100 °C [3-6,10]. R718 is one of the most attractive working fluids for heat pumps operating up to and beyond 200 °C, as it can achieve the highest condensation temperatures owing to its critical temperature at 373.9 °C. R718 also displays several other favourable properties, including zero ozone depletion, zero global warming potential, low cost, and high availability. It is chemically stable, non-toxic, and non-flammable, making it one of the safest known working fluids with no environmental impact.

The compressor is the single most critical component in HTHPs. For R718 HTHPs, research on compressors has been conducted on a wide range of oil-free compression technologies, including twin-screw [7,11], oil-free turbo [4–6], MVR-fans [10], and specialized positive-displacement machines [12], many of which have demonstrated promising performance, but also technical challenges related to mechanical integrity. Although piston compressors are widely used in industrial HTHP installations operating with both synthetic and natural working fluids [3], the combination of piston compressors and R718 has been less explored. Piston compressors offer several advantages, such as high isentropic efficiencies at both design and part-load conditions, and the ability to achieve higher stage pressure ratios and temperature lifts than dynamic compressors, partly due to the low molecular weight of R718. Provided that challenges related to material selection, sealing, and lubrication can be resolved, integrating piston compressors in R718-based HTHPs represents an attractive technological opportunity. This study contributes to this research through a steady-state and dynamic performance evaluation of a four-stage R718 HTHP. The work includes a geometric evaluation of a novel oil-free piston compressor for several HTHP concept layouts incorporating different interstage desuperheating methods. The results will be used as input to the design of the operational strategy, component dimensioning, and performance assessment of the HTHP pilot.

2. Methods

2.1. Concept evaluation of the GEOSYN high-temperature heat pump

A key objective within the GEOSYN project is to develop a high-temperature heat pump (HTHP) using R718 as the working fluid. The HTHP pilot will be designed, fabricated, and tested at the laboratory facilities of Rivacold, an Italian heat-pump supplier before being installed at S.R.M Formaggio's dairy factory in Monterotondo Marittimo, Italy. At the factory, the system will utilize geothermal heat available at approximately 125 – 140 °C and upgrade it to around 185 – 190 °C To define the starting point for the HTHP concept development, an initial set of system requirements and constraints were established, which were derived from several sources, including boundary conditions at the factory site and GEOSYN objectives. A selection of the key requirements is listed in Table 1.

Table 1. Initial set of key system requirements for concept evaluation

Parameter	Value	Comment
Maximum condenser duty	50 kW	GEOSYN HTHP objectives
Maximum cycle temperature lift	80 K	
Minimum heat source temperature	125 °C	Pilot site conditions
Heat source/sink media	Water/steam	
Minimum approach temperature between hot and cold fluid in HXs	5 K	Assumption

Based on the inputs in Table 1, the evaporating and condensing conditions at the design point are 120 °C / 1.99 bara and 200 °C / 15.5 bara, respectively. The compressor currently under development is a four-stage, oil-free piston compressor from the Italian supplier Officine Mario Dorin. It is a novel prototype developed specifically for steam. To enable oil-free operation inside the compression chambers, seals on the linear connecting rod prevent leakage of steam from the cylinders into the oil-filled crankcase. Because the compressor operates without oil in the cylinders, the piston rings are made of a self-lubricating material, and the inner cylinder surfaces are coated with a thin layer of the same material to reduce ring wear and prolong the expected lifetime. The coating is sensitive to the presence of water droplets, which can cause erosion and eventually severe damage to the compressor. Since the working fluid is R718, it is essential to operate the compressor under superheated steam conditions only and avoid any formation of condensed droplets inside the compressor during operation. To minimize the risk of droplet formation upstream of each compressor stage, a minimum suction superheat of the steam of 20 K above the saturation temperature is specified.

At the same time, the sealing material, being sensitive to high temperatures, cannot tolerate much higher than 250–270 °C. This constraint determines the maximum allowable temperature inside the compressor and consequently limits the maximum pressure ratio that can be achieved within a single compression stage. It was therefore established that a heat pump cycle consisting of four compression stages (stage 1-4) was required to avoid exceeding the maximum discharge temperature.

After each compression stage, a corresponding stage of steam desuperheating is required. The desuperheating process serves two main purposes: The first is to reduce the inlet temperature for the following compression stage, ensuring that a new round of compression can take place without exceeding the maximum discharge temperature. The second is to reduce the specific compression work, since for a given pressure ratio, lowering the compressor inlet temperature decreases the specific volume of the working fluid, resulting in a reduction of the specific work. At the same time, to avoid the risk of droplet formation at the suction side of the compressor, the desuperheating must stop once the steam reaches a temperature, corresponding to 20 K superheat at the compressor inlet. For this reason, a key element in the concept evaluation is the selection and design of a suitable desuperheating process that can maintain at least 20 K superheat at the suction at all operating conditions, minimize the risk of liquid droplets, remain low in complexity and costs, and allow robust controllability. Furthermore, it is essential to understand how the desuperheating strategy impacts the performance of the heat pump, especially the Coefficient of Performance (COP), but also the compressor geometry (bore diameter), and the stage pressure ratio.

In total, four main HTHP cycle layouts were evaluated at steady-state conditions, at the design point. All thermophysical properties were calculated using the NIST REFPROP database. A simplified schematic of these cycles is shown in Fig. 1. The four main HTHP cycle layouts all operate in the following manner: The R718 working fluid is evaporated to saturated steam in the evaporator before being compressed in four stages, followed by desuperheating after stage 1-3. After stage 4, the superheated steam is sent to the condenser, where it is condensed until saturated liquid conditions are reached. Finally, the working fluid is expanded back into the evaporator. The cycle layouts differ primarily in the method used to desuperheat the steam.

In Layout A, desuperheating is performed by liquid injection. A fraction of the pressurized saturated liquid is extracted from the condenser outlet and injected through expansion valves and spray nozzles that atomize the liquid into fine droplets, which mix with the superheated steam before the compressor inlet. The droplets evaporate rapidly and cool the superheated steam. A key advantage of this method is its simplicity and the fact that no external auxiliary coolant is required. To obtain the specified 20 K superheat after the evaporator, a fraction of the superheated steam after stage 4 is recirculated and mixed with the saturated steam upstream of stage 1. This achieves the required superheat without lowering the evaporation temperature and pressure to force fully dry evaporation inside the evaporator, which would otherwise increase the cycle pressure and temperature lift. The main drawback of Layout A is that a portion of the steam that could have contributed to heat output from the condenser must instead be recycled. As a result, a higher mass flow rate through the compressors is required to deliver the specified heat output.

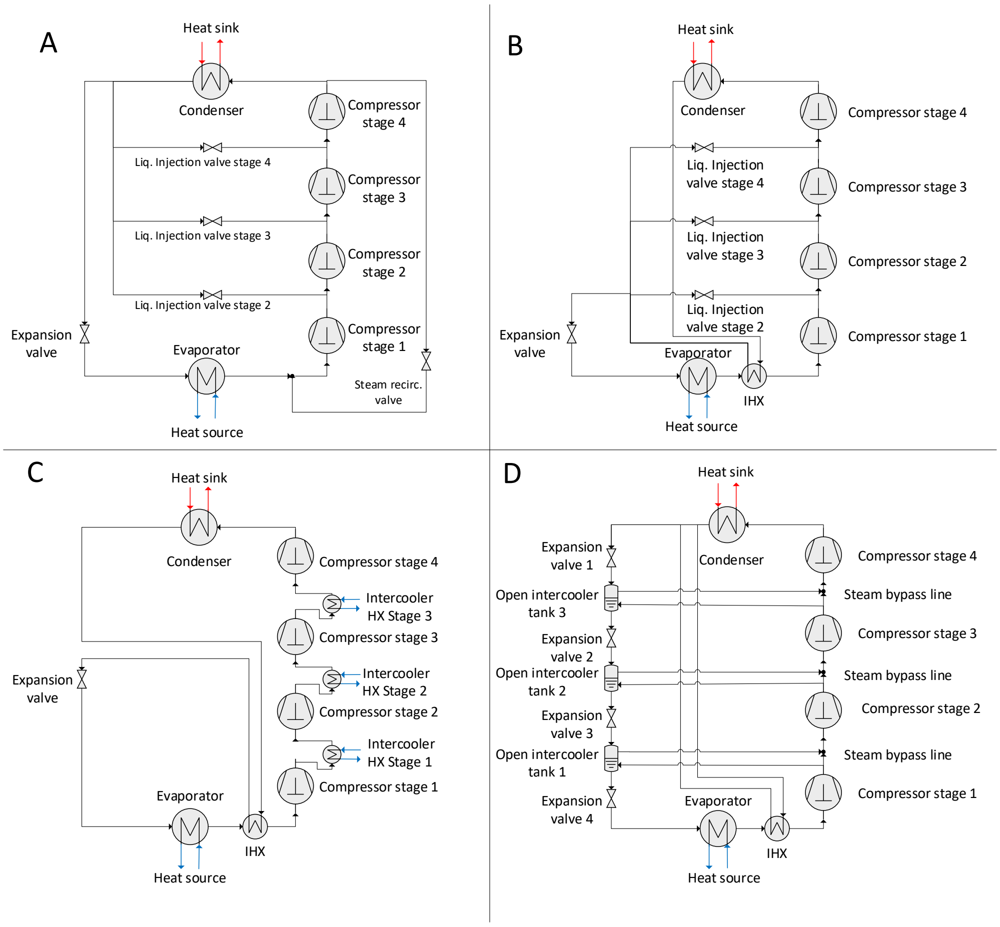

Figure 1. Schematic diagrams of the four main HTHP cycle layouts in the concept evaluation.

To address this issue, Layout B incorporates an Internal Heat Exchanger (IHX). In this layout, the superheat prior to the first compression stage is achieved using the IHX, which transfers heat internally in the HTHP from the high-pressure side to the low-pressure side. The liquid exiting the condenser is subcooled, while the saturated steam entering the first compression stage is superheated.

In Layout C, the interstage desuperheating is performed using traditional heat exchangers, which separate the R718 working fluid from an auxiliary coolant. The motivation behind this layout is to propose a concept that avoids liquid injection, thereby eliminating the inherent risk of incomplete full evaporation of the injected liquid associated with Layouts A and B. The downside, however, is that using an auxiliary coolant is that the energy transferred to the coolant during the desuperheating process is lost, unless it is used to cover other heat demands. The specified superheat at the first compression stage is managed using an IHX, as in Layout B.

Layout D features three open intercooler tanks, each operated at an intermediate pressure. The discharge gas from each compression stage is injected into the liquid-filled intercooler tank, causing full desuperheating to saturated conditions. The resulting vapor is then supplied to the suction of the next compression stage. To ensure the required level of superheat, a steam bypass line going directly from the previous stage to the next is incorporated. A total of four expansion valves is used to control the tank pressure and liquid level. An advantage of Layout D is that it enables improved economizing by utilizing all the vapor produced in the open intercooler tanks, which increases the cycle COP. In addition, the concept is inherently safe in terms of the risk of liquids entering the compressor, as the operating principle together with liquid-level control and flood protection makes it impossible for R718 in liquid form to reach the compressor. The drawback is that Layout D is that it is the most complex, both in terms of the number of components and controlled parameters.

2.2. Evaluation and selection of compressor geometry

The compressor supplied by Dorin is an open-type piston compressor with a total of eight cylinders. To account for the reduction in specific volume of the steam through each compression stage, the cylinders are distributed as follows: four cylinders for stage 1, two for stage 2, one for stage 3, and one for stage 4. The main compressor parameters and constraints are listed in Table 2. The isentropic and volumetric efficiencies are conservatively assumed values provided by Dorin. The performance of the compressor in steam environment will be demonstrated when integrated in the HTHP during the upcoming laboratory experiments.

Table 2. Compressor parameters and constraints

Parameter	Value
Number of cylinders, N_c	8
Speed range, RPM_{crank}	500–1450 [rev/min]
Isentropic efficiency, η_{is}	0.75
Volumetric efficiency, η_{vol}	0.85
Cylinder stroke length, L_s	65 mm
Maximum cylinder bore diameter, $D_{b,max}$	90 mm

As shown in Table 2, parts of the compressor geometry design are predefined by Dorin. However, the bore diameter of each stage, must be specified. Because the compressor has four compression stages, there is significant freedom in selecting the operating and geometric parameters of each stage, such as stage pressure ratios and cylinder bore diameters. The bore diameter required for a given stage is calculated based on Eq. (1):

$$D_b = \sqrt{\frac{240 \cdot \dot{V}_{in}}{\pi \cdot L_S \cdot RPM_{crank} \cdot N_{c,stage} \cdot \eta_{vol}}} \quad , \tag{1}$$

where $\dot{V}_{in}$ is the inlet volume flow rate [kg/s]. The bore diameter depends on the volume flow rate, which is in turn dependent on the inlet pressure and temperature. This means that the pressure ratio of one stage affects the inlet conditions, and thus the cylinder diameter of the next stage. Such dependencies could theoretically be eliminated by adding bypass or recirculation loops; however, this is not implemented as it would increase system complexity and reduce the COP. The selection of stage pressure ratios and bore diameters must also satisfy system constraints such as maximum discharge temperatures, condenser duty, and the bore diameter limit, while maximizing the COP. To address this, an optimization procedure was developed to determine the optimal stage pressure ratios at the design point. The COP was used as the objective function, while the pressure ratios of stages 1–3 were treated as optimization variables. The discharge temperatures of stages 1–4 were included as constraints. The pressure ratio of stage 4 was calculated directly from the outlet pressure of stage 3 and the required condensing pressure. The optimization was carried out using the Generalized Reduced Gradient (GRG) nonlinear solver, which is computationally efficient and performs well for thermodynamic systems. A known limitation of GRG is that it may converge to local optima; therefore, multiple starting points were evaluated. Fig. 2 shows a schematic decision tree summarizing the procedure.

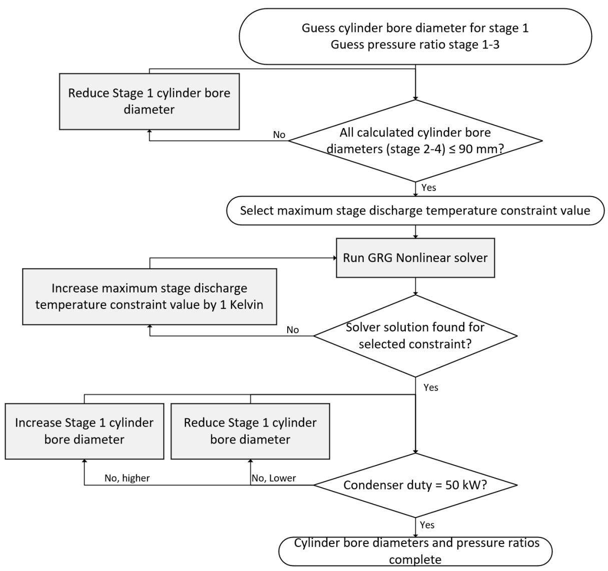

Figure 2. Procedure for selection of operating parameters (stage pressure ratio), and geometry (cylinder bore diameter).

The method begins with initial guesses for the bore diameter of stage 1 and the pressure ratios of stages 1–3. The resulting bore diameters of stages 2–4 are then checked against the 90 mm limit.

Ideally, the maximum discharge temperature would be limited to 250 °C; however, with the implementation of a high-temperature self-lubricating sealing material, discharge temperatures up to 270 °C may be tolerable. Therefore, the optimization initially imposed a 250 °C limit. If no feasible solution was found, the temperature constraint was increased in increments of 1 K until a solution was obtained. Finally, an additional iteration was performed to adjust the stage 1 bore diameter so that the resulting cycle mass flow rate provided the required thermal capacity of 50 kW.

2.3. Interstage desuperheating strategy

The desuperheating of high-temperature heat pumps can be achieved through various methods depending on the system design and operational requirements. These approaches can broadly be categorized into two different strategies: 1) methods employing direct liquid injection, and 2) methods using intercooling, either in open or closed form [13]. The direct liquid injection methodology is typically realized by integrating atomizing spray nozzles or Venturi nozzles into the primary flow path, with the injected water supplied from the process system. This strategy has a long track record in the steam process industry but differs in several important ways from its application in heat pump cycles. For example, industrial steam processes generally operate under relatively steady conditions, whereas heat pumps must operate dynamically under varying loads and boundary conditions. Additional challenges arise in designing robust flow-control strategies, particularly the need to accurately meter the injected liquid and to maintain stable operation under low-flow conditions. Although recent analytical and theoretical studies have evaluated liquid injection and the associated thermodynamics [14], the implications of integrating such strategies into physical HTHP systems remain less explored.

An alternative desuperheating approach is intercooling, which can be implemented in several ways, each with its own advantages and limitations. Interstage cooling can achieved using a closed intercooling system, in which heat exchangers placed are placed downstream of each compression stage requiring desuperheating. The auxiliary cooling loop of these heat exchangers therefore becomes an additional design variable that may vary between HTHP systems. A key benefit of this approach is the absence of liquid injection into the primary steam flow, resulting in a fully closed system design. However, this may come at the cost of added pressure drop and potential logistical challenges [6].

A second option is open intercooling, which uses liquid receivers to cool the discharge steam from each compressor stage to its saturation temperature. This concept is also widely used in industrial steam systems, but certain challenges arise when adapting it to HTHP applications. For example, cooling the steam to the saturation point inherently increases the risk of liquid droplet formation, which is a particular concern for oil-free high-temperature compressors due to the sensitivity of the cylinder coating materials. This approach was examined in the theoretical study by Andersen et al. in 2024 [15].

Overall, the design and integration of desuperheating in high-temperature heat pumps is a flexible design without a single universally optimal solution. The heat pump designer is therefore required to evaluate several desuperheating strategies in parallel, balancing thermal performance, system complexity, risk of liquid entrainments, controllability, and cost.

2.3.1. Design considerations for desuperheating implementation

The integration and design philosophy for the desuperheating system aimed primarily to minimize the risk of liquid water entering the compressor, while simultaneously satisfying the overall thermal design requirements of the HTHP. Additional factors influencing the selection included practical implementation aspects such as commercial availability, estimated cost, system complexity, and instrumentation and control requirements.

Three desuperheating methods were considered for the GEOSYN HTHP system: a) liquid injection, b) closed heat exchangers, and c) open intercooler tanks. The direct injection corresponds to Cycle Layouts A and B shown in Fig. 1, while the closed and open intercooling concepts correspond to Layouts C and D, respectively. Comparative analyses of the desuperheating methods evaluated several dimensions: risk, controllability, physical implementation aspects (including space requirements), commercial availability, and cost, and relative performance impacts on the HTHP. A summary of the key design considerations is provided in Table 3, highlighting the risk of liquid ingestion, system controllability and complexity, and the expected impact on the HTHP performance, as presented in the results.

Table 3. Key design considerations for GEOSYN desuperheating implementation

Design consideration	Liquid injection	Closed intercooling (heat exchangers)	Open intercooler tanks
Risk of liquid droplets entering the compressor	**Medium**: Possible due to liquid injection and potential condensation.	**Low–Medium**: Unlikely; potential condensation on heat exchanger surfaces.	**Low**: Vapor-liquid separation provides inherent protection, only sat. vapor flowing downstream.
HTHP performance (COP)	**Medium**: Improved cycle economizing	**Low-Medium**: Thermal energy lost through desuperheating	**High**: Full cycle economizing
Complexity	**Medium-High**: Difficult to regulate; dynamic flow control required.	**Low**: Good controllability via coolant-side regulation; only method enabling air cooling during start-up.	**Medium**: Flash tank liquid level control. Less active control achievable compared to closed intercooling.

2.4. Start-up strategy using air and introduction of steam

At start-up, all component surfaces such as the compressor, heat exchangers, piping, and valves, will be cold. Pre-charging the system with water under these conditions is not feasible. Even if steam could be instantly generated in the evaporator, the likelihood of condensation on cold internal surfaces would be high, posing a serious risk to the integrity of the compressor. For this reason, a start-up strategy was developed in which the system is preheated until temperatures close to the expected design point operational levels are reached. The selected method is to circulate air through all relevant components of the HTHP including the compressor. The mechanical work from the compression stages is transferred to the air as thermal energy, which progressively heats up the internal surfaces. Similar air-based preheating approaches have been used in other steam heat pumps experimental projects [4–6]. The strategy of pre-heating with air requires careful evaluation, since all selected components must be compatible with both steam and air across the full range of start-up conditions. One example is during compression, as air and steam exhibit different thermophysical properties, particularly the specific heat ratio $\gamma = C_p/C_v$, which strongly influences the temperature rise during compression. At the design inlet conditions of the first compression stage (2 bara, 140 ºC), air has a γ-value of approximately 1.8, compared with 1.34 for steam. Consequently, air undergoes a significantly larger temperature increase than steam for the same pressure ratio.

Initial evaluations showed that was not possible to operate the start-up sequence with air at the same inlet pressure as steam, due to the resulting stage 1 discharge temperature, which was too high. One potential alternative, reducing the pressure ratio, would require the installation of bypass valves to bleed off air between compression stages, thereby reducing the volumetric flow rates. However, this approach would add complexity in both the number of components and control requirements. A more robust and elegant solution is to reduce inlet pressure of the first compression stage to approximately atmospheric pressure during preheating. Operating at atmospheric inlet pressure reduces the pressure throughout the system to roughly 50% of the design levels seen during steam operations, and more importantly, reduces the maximum discharge temperatures within safe limits for the compressor.

The preheating phase is finalized once the temperature at the inlet stage 1-4 reaches the steam saturation temperature at the prevailing pressure plus 20 K. At this point, steam can safely be introduced into the cycle. This is done by feeding water from a pressurized tank equipped with an internal heater and a fresh make-up water supply, which also acts as a high-pressure liquid receiver during normal operation. The water is expanded through the main expansion valve, producing partial flash evaporation. Additional heating in the main evaporator, activated at this stage, ensures complete evaporation.

2.5. Dynamic modelling

A dynamic model of the HTHP and the auxiliary fluid circuits, based on concept Layout C, was developed in Dymola, a numerical simulation software based on the Modelica programming language, using components from the TIL library (TLK-Thermo GmbH). The model was simulated with both air and steam as working fluids with the aim of investigating the operational performance under all expected conditions, providing input for and validating component dimensioning (e.g., heat-exchanger area, valve Kv-values, compressor geometry), and supporting the development of an operational strategy and control approach. A graphical overview of the model is shown in Fig. 3.

All components were parametrized according to design conditions. The compression stages assume adiabatic compression with parameters from Table 2, using selected bore diameters presented in Section 3.3, and operating at 1200 rpm. Mechanical and electrical losses were neglected. All heat exchangers are modeled using plate-heat-exchanger geometry. To characterize their performance, constant heat-transfer coefficients for the cold- and hot-side fluids were specified, resulting in constant overall heat-transfer coefficients (U) and heat-transfer areas (A). The UA-values were validated against performance data provided by the heat-exchanger supplier for both air and steam operation. Each heat-exchanger model included a small pressure drop of approximately 0.2–0.5 bar, based on quadratic mass-flow-dependent pressure-drop correlations. All valves were parametrized using Kv-values, and heat losses from all components were neglected.

The secondary-fluid circuits were modelled according to the planned configuration in Rivacold's laboratory and therefore differ slightly from the setup at the pilot site. All circuits operate with water/steam as the working fluid. The heat-sink, heat-source, and desuperheating-coolant circuits were kept hydraulically separated to avoid interdependence in the control of process conditions.

A control strategy has been implemented to regulate the process conditions in both the HTHP cycle and the secondary circuits. PI controllers regulate the conditions according to fixed or variable operating setpoints. The suction superheat of stage 1 is controlled by adjusting the valve opening (Kv-value) of the cycle expansion valve. The suction superheat of stages 2-4 is controlled individually using three separate 3-way valves in the auxiliary desuperheating coolant circuit, which regulate the water mass flow rate entering the desuperheater heat exchangers. To ensure no condensation of steam on the heat-exchanger walls during desuperheating, the coolant water inlet temperature was maintained at 140–160 ºC (depending on stage) and pressurized to 9 bara. These conditions ensure small temperature differences while keeping the wall temperature above the steam saturation temperature at all times.

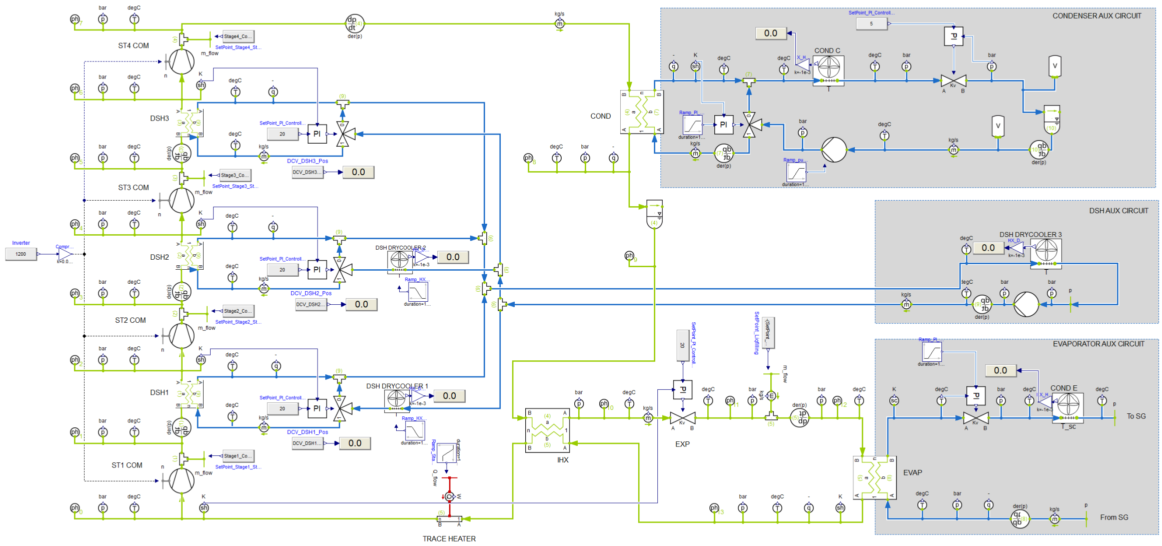

Figure 3. Full Dymola model of the GEOSYN HTHP, including auxiliary circuits.

The heat supplied to the HTHP cycle in the evaporator is provided by a steam generator that produces steam at 143 ºC / 3.9 bar, consistent with field measurements at the pilot site. The mass flow rate of steam in the auxiliary heat-source circuit is regulated using a throttling valve downstream of the evaporator. On the sink side, the auxiliary circuit is modelled using a pump that delivers pressurized water to a 3-way valve, which regulates the coolant mass flow entering the condenser. Since the HTHP will deliver steam at the pilot site, the system is designed such that the condensation of the working fluid causes the coolant water to evaporate. At the design point, the regulation setpoint for the outlet conditions is 181 °C / 9 bara.

The control system then ramps up the evaporating and condensing temperatures and pressures of the HTHP cycle following the air-based preheating phase until the design conditions are reached. The cycle is controlled indirectly through dynamic temperature and pressure regulation of the heat-source and heat-sink circuits. On the heat-sink circuit, ramp-up is achieved by simultaneously increasing the outlet pressure of the pump and the superheat temperature of the produced steam via the 3-way valve. On the heat-source side, the outlet temperature of the auxiliary fluid from the evaporator is increased by regulating the throttling valve.

For the desuperheaters, the inlet temperature of the coolant is actively controlled and gradually increased during ramp-up. Combined with the use of co-current (rather than counter-current) heat-exchanger configurations, this ensures that the coolant remains in the liquid phase under all operational conditions.

A key motivation behind implementing dynamic temperature and pressure control on the auxiliary circuits is to avoid large variations in mass flow rates during pre-heating and steam ramp-up, which would make the selection and dimensioning of suitable components considerably more difficult.

3. Results and Discussion

3.1. Results from initial steady state evaluations

HTHP concept Layouts A–D were initially evaluated at design point conditions following the developed optimization procedure. In this evaluation, the compressor speed was set to 1450 rpm, while the isentropic and volumetric efficiencies (η_{is} and η_{vol}) were assumed to 0.75 and 1, respectively. The suction superheat at each compressor-stage inlet was specified to 20 K, and pressure drops between stages were neglected. The results of the evaluation are shown in Fig. 4.

For all concepts, the solver identified feasible optimal solutions that satisfied the constraints on maximum bore diameter (90 mm), maximum stage discharge temperature (250 °C), and condenser duty (50 kW). The optimal cylinder bore diameters vary significantly between the different layouts.

Layout A achieved the lowest performance, with a COP 3.4, corresponding to approximately 50% Carnot efficiency (assuming sink and source temperatures of 195 °C and 125 °C, respectively). Performance improves substantially in Layout B, where the stage-1 superheat is obtained using the IHX rather than gas recirculation. This reduces the inlet mass flow rate to stage 1 by 16% (from 85.1 to 71.6 kg/h), resulting in noticeably smaller bore diameters across all compression stages.

In Layout C, the performance decreases compared with Layout B, primarily because the heat removed during desuperheating is not recovered. Furthermore, Layout C is the only concept in which the mass flow remains constant through all compression stages, as neither liquid injection nor open intercooling is applied. Consequently, the required mass flow rate in the early compressor stages is higher than in the other layouts, which is reflected in larger bore diameters in the first stages.

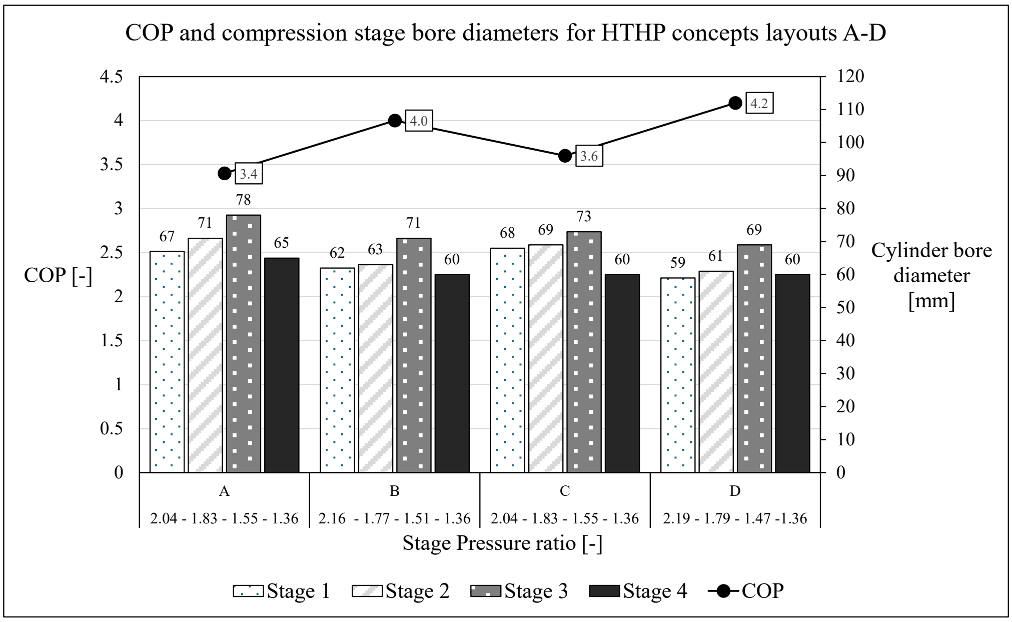

Figure 4. Steady-state simulation results showing COP, cylinder bore diameters, and stage pressure ratios for concept Layouts A–D.

The highest performance is achieved with Layout D, with a COP of 4.2, corresponding to a Carnot efficiency of approximately 63%. The economizing effect from the open intercooling tanks provides an even greater benefit than liquid injection, reducing both the mass flow and the corresponding compressor duty in the first three compression stages.

The pressure ratios for each stage are also shown in Fig. 4. In principle, multi-stage compression cycles achieve highest efficiency when the pressure ratio is evenly distributed across all stages. However, due to the discharge-temperature limitation, this was not feasible here. Instead, the optimal pressure ratio is highest for the first stage and decreases progressively in the subsequent stages.

3.2. Selection of heat pump cycle and final steady-state evaluation

Based on the performance evaluation and the interstage desuperheating design considerations, Layout C was selected as the final HTHP concept for GEOSYN. Layout B demonstrated high thermodynamic performance during the evaluation. However, as the project progressed, a combination of previous experimental experience at SINTEF [4,5] and updated information from ongoing discussions with suppliers of liquid-injection systems increasingly indicated an elevated risk of liquid-water droplet presence under certain operating conditions. Layout D, on the other hand, showed promising results in terms of both performance and reduced droplet risk. Nevertheless, in the final phase of the concept assessment, the project partners considered this layout to be overly complex, due to the increased number of components and associated control requirements, which ultimately reduced its suitability for implementation. Among the evaluated configurations, Layout C offered the most favourable balance between system complexity, operational risk, and performance. An additional advantage is that during the air-based preheating phase, the use of conventional heat exchangers provides a more straightforward method of preheating. The coolant flow can be activated to limit air temperatures prior to each compression stage, which improves operational robustness.

A final steady-state evaluation of Layout C was performed, incorporating additional parameters. These included a 5% pressure drop in each of the desuperheating heat exchangers, a reduced volumetric efficiency (η_{vol}=0.85), and steam-leakage rates per stage to account for expected compressor leakage. The compressor speed at design conditions was reduced to 1200 rpm to improve long-term durability.

Because the cylinder bore diameters obtained from the initial steady-state evaluation were not compatible with standard machining tolerances, and given the revised set of parameters, several alternative bore-diameter configurations were evaluated based on proposals from Dorin, using a revised version of the optimization procedure described in section 2.2. Table 4 summarizes the key results for three candidate options. The results show minor differences in COP between the three options. However, the maximum discharge temperatures increased from the initial evaluation and varying significantly, with the worst case occurring for Option 3, where the stage 4 temperature reached 283 °C. Option 2 was ultimately selected, as it provided a slight improvement in both COP and thermal capacity compared with Option 1, while still maintaining all discharge temperature below the acceptable limit of 270 °C.

Table 4. Performance evaluation for Layout C under different cylinder-bore configurations.

	Option 1				Option 2				Option 3			
Parameter	D_b [mm]	$T_{\mathrm{discharge}}$ [°C]	PR [-]	$\dot{V}_{\mathrm{swept}}$ [m^3/h]	D_b [mm]	$T_{\mathrm{discharge}}$ [°C]	PR [-]	$\dot{V}_{swept}$ [m^3/h]	D_{b} [mm]	$T_{\mathrm{discharge}}$ [°C]	PR [-]	$\dot{V}_{\mathrm{swept}}$ [m^3/h]
Stage 1	80	249	2.18	80.0	80	249	2.17	80.0	75	228	1.90	70.3
Stage 2	80	240	1.70	40.0	80	240	1.70	40.0	80	234	1.70	40.0
Stage 3	90	258	1.68	25.3	90	245	1.54	25.3	90	239	1.54	25.3
Stage 4	72	257	1.46	16.2	75	267	1.60	17.6	75	283	1.83	17.6
COP [-]	3.33				3.36				3.43			

Operational parameters: T_{evap}: 120 °C, T_{cond}: 200 °C, compressor speed: 1200 rpm, η_{is}: 0.75, η_{vol}: 0.85, interstage pressure drop: 5%, steam leakage rate: 1.20% (Stage 1), 0.6% (Stage 2), 0.3% (Stage 3), 0.3% (Stage 4)

3.3. Results from dynamic modelling with air and steam

The dynamic simulation model was evaluated using air and steam in two separate simulations. Key compressor-related result parameters from both simulations are shown in Fig. 5. The first half (14 000 seconds) of the simulation window corresponds to the air-preheating phase, while the second half represents operation with steam during the ramp-up period until design-point conditions are reached. The top diagram (a) shows the discharge temperatures from stages 1-4. Throughout the entire simulation, the temperatures remain below the 270 °C limit, reaching a maximum of 267 °C at the design point, consistent with the steady-state evaluation. During the air-preheating and steam ramp-up phases, the discharge temperatures are lower because of the reduced inlet pressures, ranging between 200–250 °C. During air-preheating, the stage 1 inlet temperature starts at 20 °C, gradually increasing to 120 °C towards the end as shown is the bottom diagram (b). The stage 1 discharge temperature follows a similar trend. Because the dynamic evaluation was conducted as two separate simulations with different working fluids, a discrete transition in the result parameters occurs at the point where the model switches from air to steam.

During the simulation with steam, the control system, supported by active variation of desuperheating coolant inlet temperatures to avoid large changes in coolant mass flow rate, successfully maintained the specified superheat of 20 K at all stage inlets. COP at the design point was 3.35, consistent with the steady-state evaluation.

Regulation of the heat-sink and heat-source pressure and temperature set points, used to indirectly control the evaporating and condensing conditions of the HTHP cycle, was demonstrated successfully. The minimum (stage-1 suction) and maximum (stage-4 discharge) cycle pressures remained stable throughout the simulation, as shown in the bottom diagram (b). However, several iterations were required to identify suitable dynamic ramping trajectories. Future work will therefore investigate combining dynamic setpoints with direct regulation techniques to simplify and improve the robustness of the control strategy.

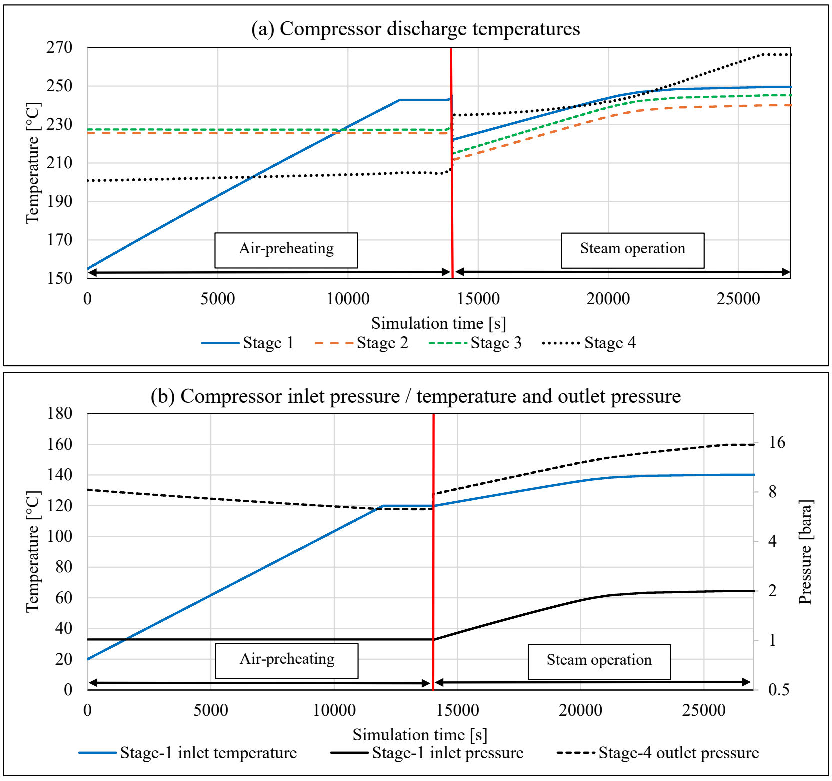

Figure 5. Key result parameters from the dynamic simulation.

4. Conclusions

This work presents the performance assessment and geometric analysis of a novel oil-free four-stage piston compressor for a HTHP operating with R718 as the working fluid, delivering an 80 K temperature lift and condensing at 200 °C / 15.5 bara. The geometric analysis resulted in suitable bore diameters and pressure ratios that satisfied the maximum discharge-temperature constraint for all evaluated HTHP concept layouts. However significant variations between the layouts were identified, demonstrating the strong interdependence between the cycle layout and compressor design. The qualitative assessment of interstage desuperheating strategies, together with the steady-state performance analysis, showed that the concept employing closed intercooling (Layout C) using traditional heat exchangers offers the most favourable compromise between performance, system complexity, and operational robustness. With the final selected bore diameters, Layout C achieved a COP of 3.36. The air-preheating strategy, necessary to avoid the presence of liquid in the compressor during cold start-up, was shown to be feasible when operating at reduced inlet pressures. Dynamic simulations of both the air-based preheating phase and the subsequent steam operation confirmed the viability of the selected layout, the operational strategy, and the implemented control methodology. During steam operation, the simulations demonstrated stable control of stage-superheat levels and pressure profiles, achieving COP values consistent with steady-state predictions. Overall, the findings support the design and implementation of the GEOSYN HTHP pilot, providing a validated basis for further work on component sizing and selection, control strategy development, operational management, laboratory validation, and performance evaluation under real industrial operating conditions at the pilot site.

Acknowledgements

This research has received funding from Horizon Europe under the grant agreement No. 101172812 (Project: GEOSYN).

References

[1] IEA, 2019, Renewables 2019, IEA, Paris https://www.iea.org/reports/renewables-2019
[2] Arpagaus, C., Bless, F., Uhlmann, M., Schiffmann, J., and Bertsch, S. S., 2018. High temperature heat pumps: Market overview, state of the art, research status, refrigerants, and application potentials, Energy, vol. 152, pp. 985–1010, 2018, https://doi.org/10.1016/j.energy.2018.03.166.
[3] Zühlsdorf B., et al., IEA HPT Annex 58 — High-Temperature Heat Pumps, 2023. Task 1 (Technologies) report, Annex 58 Task Report. https://heatpumpingtechnologies.org/annex58/wp-content/uploads/sites/70/2023/09/annex-58-task-1-technologies-task-report.pdf. HPT - Heat Pumping Technologies
[4] Bantle, M., Schlemminger, C., Gabrielii, C., and Ahrens, M., 2019. Turbo-compressors for R-718: Experimental evaluation of a two-stage steam compression cycle https://doi.org/10.18462/iir.icr.2019.0973.
[5] Dowdell, J. R., Moen, O. M., Rotan, M., Schlemminger, C., 2024. Development, experimental testing, and performance analysis of a two-stage steam turbo compressor HTHP for solar assisted heat supply. 16th IIR-Gustav Lorentzen Conference on Natural Refrigerants - GL2024: Proceedings. https://doi.org/10.18462/iir.gl2024.1286
[6] Kriese, M., Klöppel, S., Setzepfand, N., Schaffrath, R., & Nicke, E., 2023. Part-Load Behavior and Start Up Procedure of a Reverse Rankine High Temperature Heat Pump With Water As its Working Medium, Turbo Expo: Power for Land, Sea, and Air. American Society of Mechanical Engineers. https://doi.org/10.1115/GT2023-103410
[7] Hamid, K., Ren, S., Tolstorebrov, I., Hafner, A., Sajjad, U., Arpagaus, C., Moen, O.M., and Eikevik, T. M., Experimental optimization of an absorption-compression heat pump with wet compression for large temperature glide industrial applications, Renewable Energy, Volume 243, 2025, 122531, ISSN 0960-1481, https://doi.org/10.1016/j.renene.2025.122531
[8] PUSH2HEAT, Publications, https://push2heat.eu/. https://push2heat.eu/project-materials/publications/ (accessed Nov 17th 2025)
[9] SPIRIT, Publications, https://spirit-heat.eu/. https://spirit-heat.eu/project-materials/publications/ (accessed Nov 17th 2025)
[10] Bantle, M., Schlemminger, C., Nilsen, V., 2024. Integration of a 1.6 MW steam supplying heat pump into feed production process. 4th High-temperature Heat Pump Symposium: Book of Presentations. DTU Mechanical Engineering. https://orbit.dtu.dk/en/publications/4th-high-temperature-heat-pump-symposium-book-of-presentations/
[11] Chamoun, M., Rulliere, R., P. Haberschill, and J. L. Peureux, 2014. Experimental and numerical investigations of a new high temperature heat pump for industrial heat recovery using water as refrigerant, Int. J. Refrig., vol. 44, pp. 177–188, https://doi.org/10.1016/j.ijrefrig.2014.04.019.
[12] SINTEF, Free2Heat project, https://sintef.no. https://www.sintef.no/en/projects/2019/free2heat/ (accessed Nov 17th 2025)
[13] Zühlsdorf, B., Schlemminger, C., Bantle, M., Evenmo, K., & Elmegaard, B., 2018. Design recommendations for R-718 heat pumps in high temperature applications," 13th IIR Gustav Lorentzen Conference on Natural Refrigerants. International Institute of Refrigeration. http://dx.doi.org/10.18462/iir.gl.2018.1367
[14] Hosseinnia, S. M., Amiri, L., Nesreddine, H., Monney, D., & Poncet, S., 2024. Thermodynamic analysis of high temperature cascade heat pump with R718 (high stage) and six different low-GWP refrigerants (low stage), Case Studies in Thermal Engineering, 53, 103812.
[15] Andersen, M. P., Zühlsdorf, B., Markussen, W. B., Jensen, J. K., & Elmegaard, B., 2024. Selection of working fluids and heat pump cycles at high temperatures: Creating a concise technology portfolio. *Applied Energy*, *376*, 124312.